Collective Accelerator for Electrons

Richard J. Briggs
University of California, Lawrence Livermore National Laboratory, Livermore, California 94550
(Received 22 March 1985)

A concept for collective acceleration and focusing of a high-energy electron bunch is presented. The scheme combines an intense relativistic electron beam propagating in low-density gas with a trailing picosecond laser pulse for prompt photoionization of the gas to create the intense collective fields.

PACS numbers: 29.15.Dt, 41.80.Dd, 52.75.Di

Recognition of the very large space-charge electric fields produced by intense relativistic electron beams has motivated a long-standing quest for ways to utilize these collective fields for particle acceleration. The collective acceleration scheme described in this paper looks interesting for the linac collider approach to the next generation of teraelectronvolt-level high-energy physics machines.[1]

The idea is schematically illustrated in Fig. 1. The moderate-voltage, high-current "charging beam"[2] propagates in a low-density gas ($\sim 10^{13}$ to 10^{14} cm^{-3}) in the so-called "ion-focused regime," experimentally demonstrated to be a very stable self-focused beam transport mode.[3] If necessary, the propagation of the charging beam can be aided by a uv laser that weakly photoionizes the gas ahead of the beam,[4] but the majority of the ions at the end of the charging beam pulse are made by impact ionization. The intense radial electric field of the charging beam removes plasma electrons as soon as they are created; with a very abrupt tail on the charging beam an unneutralized ion column "wake" of line density comparable to the charging beam density emerges from the rear as shown. A picosecond laser pulse follows the charging beam by a time delay too short for the ions to disperse radially ($\lesssim$ 1 ns for typical parameters). This laser pulse photoionizes the surrounding gas to line densities comparable to, or greater than, the ion column line density. The inward flow of plasma electrons to neutralize the ion column's space charge creates a large axial electric field "spike" that accelerates the high-energy electron bunch as shown in Fig. 1. This pattern of plasma creation and electron flow moves axially in synchronism with the picosecond laser pulse at the speed of light, and so the acceleration field keeps in step with the high-energy electron bunch. The positive space charge on the axis also creates a radial focusing force on the high-energy bunch.

Analysis of charging beam.—If we neglect for now the gradual changes in charging beam parameters with propagation distance, and take $v_z \approx c$, all variables are functions only of $\tau = t - z/c$ and r. Maxwell's equations in cylindrical coordinates can then be shown to reduce to (mks units)

$$\partial E_z/\partial r = \eta J_r, \tag{1}$$

$$r^{-1}\partial(rH_\phi)/\partial r = \epsilon_0 \partial E_z/\partial \tau + J_z, \tag{2}$$

$$\partial(E_r - \eta H_\phi)/\partial \tau = -J_r/\epsilon_0, \tag{3}$$

with $\eta = (\mu_0/\epsilon_0)^{1/2} = 377\ \Omega$. The charging beam is focused by ions, both the (small) initial ionization from the guiding laser and the beam-generated ionization. The beam radius is a decreasing function of τ with constant emittance, but we will use a simple constant-radius model for our analysis. Since the

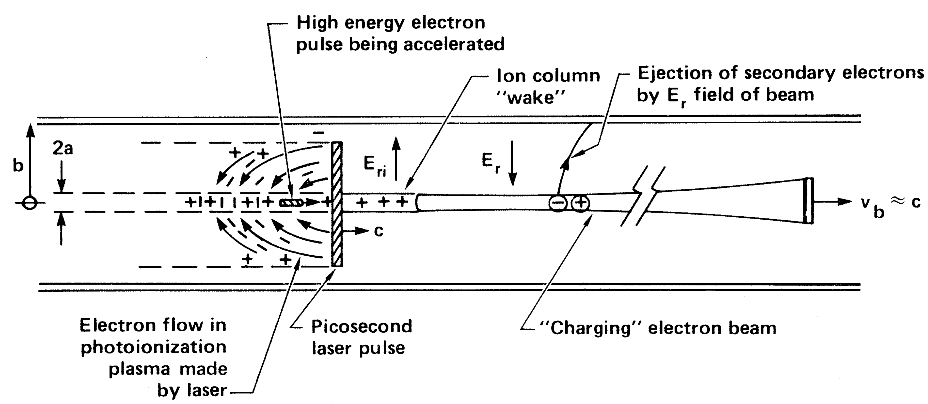

FIG. 1. Schematic of collective accelerator concept.

secondary (plasma) electrons' escape time to the wall ($\sim b/c$) is much shorter than the pulse duration, net (ion) charge density inside the beam (n_i) builds up according to[5]

$$\partial n_i/\partial\tau = \nu_d n_b \tag{4}$$

with ν_d the *direct* impact ionization rate by beam electrons and n_b the electron beam density. We take a Bennett profile for $n_b(r)$, or a current density

$$J_b = ecn_b = I_b a^2/[\pi(a^2+r^2)^2], \tag{5}$$

with I_b the beam current and a the scale radius. We use charge conservation to get the radial current density due to the radial expulsion of plasma electrons, and thus obtain E_z from Eq. (1) as

$$E_z = -\frac{\mu_0\nu_d I_b}{4\pi}\ln\left(\frac{b^2+a^2}{r^2+a^2}\right), \tag{6}$$

where we used the boundary condition $E_z=0$ at $r=b$. Note that (except at the very front tip of the beam) the deceleration rate of the charging beam is constant in τ, which means it is *uniformly distributed* over all the electrons in the pulse. We define a fractional neutralization parameter f_e *at the beam tail* by f_e = (ion line-charge density)/(electron-beam line-charge density); for our simple model $f_e = \nu_d\tau_p$ with τ_p the pulse length. It is straightforward to show that the energy per unit length lost by the charging beam ($W_b = \int E_z J_b 2\pi r\,dr$) goes into electrostatic field energy per unit length associated with the ion cloud "wake" ($\int \epsilon_0 E_r^2 \pi r\,dr = W_i$) and the kinetic-energy flux of electrons per unit length hitting the wall (W_e), with the result $W_i = (f_e/2)W_b$ and $W_e = (1-f_e/2)W_b$.

Since the collective acceleration mechanism depends on the collective electric field of the ion column, we would like to maximize f_e. Note that the gas pressure is the main experimental parameter used to vary f_e with a given τ_p. For example, in benzene, to reach $f_e \approx 1$ at the end of a 50-nsec beam pulse requires a gas density around 10^{14} cm^{-3} when beam-generated ionization is dominant[4] (and somewhat less when ion dynamics is included).[5] A conservative limit on f_e is set by the requirement that all secondary electrons made by impact-ionization events reach the wall. From a calculation of the electron orbits in the fields E_r, H_ϕ of the partially neutralized beam,[6] this will occur even for an electron starting at rest near the axis if

$$\frac{I_b}{I_0}\ln\left(\frac{b^2}{a^2}+1\right) \leq \frac{(1-f_e)}{f_e(1-f_e/2)}, \tag{7}$$

where $I_0 = 17$ kA. For example, with a 10-kA beam current and $b/a=3$, the limiting value of f_e is 0.5, corresponding to an ion line density of 10^{12}/cm at the beam tail and 25% of the energy per unit length extracted from the charging beam left behind as electric field energy.

To generate the required "sharp tail" on the charging beam, it can be sent initially through a very low-density gas pressure cell where (another) picosecond laser pulse, moving parallel to and offset from the beam axis, ionizes a plasma column that deflects away the "slow tail" characteristic of most high-current induction or pulse-line accelerators.[2] Once created, this sharp tail will broaden as the beam propagates in the collective accelerator tube since the beam electrons at the tail have a distribution of transverse velocities with a characteristic width[7] $v_\perp^2/c^2 \simeq f_e I_b/\gamma I_0$ (where γ is the beam electron energy in rest-mass units). After a propagation distance L, the electron-beam's tail will smear out over a time scale $\tau_s \sim L v_\perp^2/2c^3$. The time scale for ions to disperse radially after the beam passes is obtained from the ion oscillation dynamics in the beam's space-charge potential as $\tau_i \sim (MI_0/2m_e I_b)^{1/2} a/c$, where M/m_e is the ratio of ion mass to electron mass. Requiring that $\tau_i > \tau_s$ sets a limit

$$L < \frac{\gamma a}{f_e}(2M/m_e)^{1/2}(I_0/I_b)^{3/2}, \tag{8}$$

after which the tail would need to be "resharpened." For example, this length is of order 240 m for benzene[4] with $a \simeq 1$ mm, $I_b = 10$ kA, $f_e = 0.5$, and $\gamma = 100$.

The radial dimensions of the ion column are controlled by the normalized emittance (ϵ_n) of the charging electron beam, since the beam radius at the tail is[7]

$$a_b = \epsilon_n (I_0/\gamma f_e I_b)^{1/2}. \tag{9}$$

The 1-mm radius in this example requires an rms emittance $\epsilon_n \lesssim 0.5\pi$ rad-cm and better emittances than this have been achieved on Advanced Test Accelerator.[2]

Acceleration and focusing fields.—The mechanism for creation of an axial acceleration field following the prompt photoionization of the gas surrounding the ion column is clear from Eq. (1): The plasma electrons produced by the laser are accelerated towards the axis by the ion-column space charge, creating an outward radial current and a negative E_z pulse.

An analytic treatment is possible for a simple model where the laser pattern fills the tube, producing a uniform plasma density n_s much larger than the ion-column density (n_i). We can then treat the plasma currents (J_s) in the linear cold-fluid approximation,

$$\partial \mathbf{J}_s/\partial\tau = \epsilon_0\omega_p^2 \mathbf{E}, \tag{10}$$

where $\omega_p^2 = e^2 n_s/\epsilon_0 m$. The calculation of the fields following instantaneous plasma generation at $\tau = 0$, with an initial charge imbalance given by $en_i(r)$, is similar to the calculation of the electromagnetic fields in the "plasma wake field" accelerator.[8,9] We now use a *uniform*-density ion-column model, for simplicity, where n_i is constant inside $r=a<b$. For $\tau \geqslant 0$, the solution of Eqs. (1) through (3) with currents given by Eq. (10) gives $E_z = -E_{z0}(r)\sin\omega_p\tau$, $E_r = E_{r0}(r)\cos\omega_p\tau$, and H_ϕ *constant* in τ (a step function at $\tau=0$). Letting $E_{ri} = \rho_0 a/2\epsilon_0$ stand for the peak radial field of the ion column (with $\tau<0$), we have

$$E_{z0} = 2E_{ri}\{1/ka - I_0(kr)[K_1(ka) + K_0(kb)I_1(ka)/I_0(kb)]\}, \tag{11}$$

$$E_{r0} = 2E_{ri}I_1(kr)[K_1(ka) + K_0(kb)I_1(ka)/I_0(kb)], \tag{12}$$

$$\eta H_\phi = E_{r0}(r) - E_{ri}r/a, \tag{13}$$

in $r \leqslant a$, where $k=\omega_p/c$. In Fig. 2, we show E_{z0}/E_{ri} as a function of ka for $b \gg a$. There is a broad maximum in E_{z0} equal to $0.8E_{ri}$ around $ka \approx 1$. With $I_b = 10$ kA, $f_e = 0.5$, and $a = 1$ mm, a plasma density of several times 10^{13} cm^{-3} would therefore give acceleration fields of 2.5 MeV/cm according to this model. Examples with smaller charging beam radii, larger beam currents, and higher plasma densities will give much higher gradients than this representative parameter set. Limitations embodied in Eqs. (7)–(9) and practical constraints such as laser fluence will be the ultimate determinants on the optimized gradient.

The radial focusing force on the high-energy beam electrons is $-e(E_r - \eta H_\phi)$. At the time of peak E_z, $\omega_p\tau = \pi/2$, this radial force near the axis is always focusing, and it is approximately equal to the "bare" ion cloud field $E_{ri}r/a$ when $ka > 1$ (see Fig. 3). The strength of this focusing field for typical Stanford Linear Collider parameters[1] gives a high-energy beam radius of the order of 10 μm.

We have not considered the applicability of this scheme for acceleration of positrons in any detail; however, we note that the axial electric field is suitable for positron acceleration in the second phase of the plasma oscillation ($\pi < \omega_p\tau < 2\pi$). The radial focusing force is appropriate for positrons over part of this cycle if $ka < 1.25$; with $ka \ll 1$ most of the phase region from $\omega_p\tau = \pi$ to $3\pi/2$ is focusing (see Fig. 3).

Discussion and conclusions.—Optimum choices of plasma density and laser configuration, and predictions of efficiency and energy spread, will require more detailed analyses. We note, however, that with the right plasma density profile a high-energy beam line density exceeding the ion-column line density could decelerate plasma electrons back to low velocities as the ion column becomes neutralized. With this optimum "beam loading," a significant fraction of the electrostatic field energy of the ion column might be extracted by the high-energy beam.

The ionization energy that must be supplied by the picosecond laser is relatively modest; for example, to create a plasma line density of 10^{13}/cm requires about 2–3 J/km. The ionization and excitation processes with intense picosecond laser pulses form, in fact, a subject of considerable interest at present, and it appears that very strong ("anomalous") multiphoton ionization processes may allow a wide range of choices of gas types and laser wavelengths.[10] The technology for producing these short laser pulses at the required fluences appears to be a reasonable extrapolation of current capabilities.

Limitations of the length of a "single stage" of this accelerator concept are set by the "smearing out" of the charging-beam tail discussed earlier, the diffraction and absorption of the laser pulse, and the energy loss of the charging beam. All of these processes allow lengths of order 100 m or greater for the nominal parameters we have used. Note that the charging beam can be reaccelerated *in situ* as it propagates by addition of induction cores around the tube, and it may

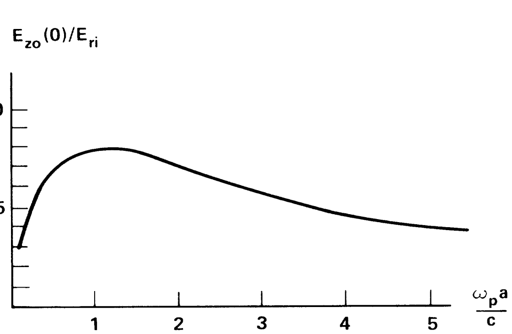

FIG. 2. Peak acceleration field on axis vs $\omega_p a/c$; E_{ri} is the peak radial electric field of the ion column.

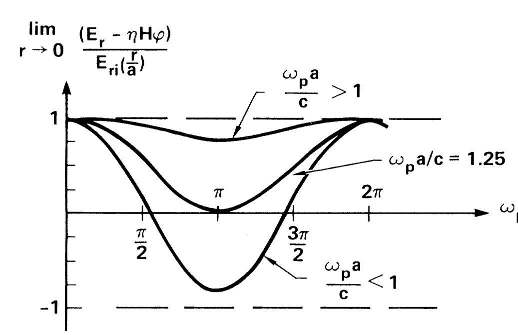

FIG. 3. Focusing force near the axis vs ω_p for different values of $\omega_p a/c$.

also be possible to place laser amplifier sections directly in the beam line to regenerate the picosecond pulse in a manner that maintains the timing of the picosecond laser pulse with the high-energy beam (which clearly must be very precise). "Resharpening" of the charging beam's tail could also be done periodically "on line"; reforming the tail would also prevent "overtaking" of the charging beam's tail by the laser and high-energy beam pulses.

A very attractive feature of the present concept relative to the plasma wake field accelerator[8,9] is the large ratio between the deceleration rate of the charging beam [$E_z \sim \mu_0 f_e I_b / 2\pi \tau_p \sim 20$ keV/m for $\tau_p = 50$ ns, $f_e = 0.5$, $I_b = 10$ kA] and the acceleration of the high-energy beam at a rate of several megaelectronvolts per centimeter (a factor of 10^4). The basic simplicity of the system should also make it a relatively inexpensive approach to a high-energy linac-collider.

Many people at Lawrence Livermore National Laboratory have contributed to the electron-beam and laser guiding ideas that underlie this concept. I would like particularly to thank Simon Yu for many useful discussions. This work was performed jointly under the auspices of the U.S. Department of Energy by Lawrence Livermore National Laboratory under Contract No. W-7405-ENG-48 and for the Department of Defense under Defense Advanced Research Projects Agency ARPA Order No. 4395, monitored by Naval Surface Weapons Center under Document No. N60921-84-WR-W0095.

[1]P. B. Wilson, IEEE Trans. Nucl. Sci. **28**, 2742 (1981).

[2]Beams from induction machines like the Experimental Test Accelerator and the Advanced Test Accelerator are what we have in mind: 5–10-kA currents, 30–50-ns pulse length, at 5–50 MeV. See for example, L. Reginato, IEEE Trans. Nucl. Sci. **30**, 2763 (1983).

[3]K. W. Struve, E. J. Lauer, and F. W. Chambers, in *Proceedings of the Fifth International Conference on High Power Particle Beams,* edited by Richard Briggs and Alan J. Toepfler (Lawrence Livermore National Laboratory, Livermore, California, 1984), p. 408.

[4]W. E. Martin, G. J. Caporaso, W. M. Fawley, D. Prosnitz, and A. G. Cole, Phys. Rev. Lett. **54**, 685 (1985).

[5]The ions will oscillate inside the beam with kinetic energies comparable to the space-charge potential (several hundred kilovolts) if the pulse length is long enough; these ions can contribute significant additional ionization later in the beam pulse. The inclusion of this process will modify the charging beam's energy-loss profile somewhat, and lower the desired operating pressure, but will not affect the general conclusions of our simple model where the ions are assumed stationary.

[6]R. J. Briggs and S. S. Yu, Lawrence Livermore National Laboratory Report No. UCID-19399, 1982 (unpublished).

[7]E. P. Lee, Phys. Fluids **19**, 60 (1976).

[8]P. Chen, J. M. Dawson, R. W. Huff, and T. Katsouleas, Phys. Rev. Lett. **54**, 693 (1985).

[9]R. D. Ruth, A. W. Chao, P. L. Morton, and P. B. Wilson, Stanford Linear Accelerator Center Report No. SLAC-PUB-3374, 1984 (unpublished).

[10]T. S. Luk, H. Pummer, K. Boyer, M. Sahidi, H. Egger, and C. K. Rhodes, Phys. Rev. Lett. **51**, 110 (1983).